Int. J. Multiphase Flow Vol. 18, No. 2, pp. 249–271, 1992
Printed in Great Britain.

0301-9322/92 $5.00 + 0.00

VALIDATION OF A ONE-DIMENSIONAL WAVE MODEL FOR THE STRATIFIED-TO-SLUG FLOW REGIME TRANSITION, WITH CONSEQUENCES FOR WAVE GROWTH AND SLUG FREQUENCY

C. J. Crowley, G. B. Wallis and J. J. Barry
Creare Inc., P.O. Box 71, Hanover, NH 03755, U.S.A.

(Received 9 May 1990; in revised form 25 October 1991)

Abstract—A one-dimensional wave model for incompressible flows predicts the transition between the stratified and slug flow regimes in pipes. The one-dimensional wave theory contains less empiricism than the commonly used Taitel–Dukler model for this transition. The empiricism embodied in the Taitel–Dukler analysis leads to the underprediction of the transition velocity at high gas density in large pipes in particular. This paper presents a complete solution methodology for the one-dimensional wave approach for this transition and validates the method by comparison with a wide range of flow regime data at large pipe diameters, at high gas density and in horizontal or inclined pipes. The analysis is extended, by using the method of characteristics, to model wave growth, decay and interaction. Since all waves usually propagate downstream we are led to question the Taitel–Dukler model for slug frequency and to suggest that the inlet characteristics, including compliance, play a role.

Key Words: flow regimes, stratified, wave theory

1. INTRODUCTION

The prediction of flow regime transitions has been studied extensively over the past two decades. Knowledge of the flow regime is a necessary prerequisite to hydraulic and thermal calculations. Knowing whether the flow regime is stratified or slug is of particular interest to the design and operation of gas and oil pipelines. It is necessary to be able to predict the effects of inclination, gas density and large pipe diameter for these pipelines.

Prior to 5 years ago, work on this regime transition was generally at low gas density (with air and water near atmospheric pressure) and at small pipe diameters (<0.05 m). Within the past 5 years, experimental data have become available at test conditions which are more prototypical of operating pipelines. This has led to the development of increasingly refined and sophisticated methods for the prediction of flow regimes.

The basis of the model described here for the regime transition between stratified and slug flows is the one-dimensional wave theory for two-phase flows. Wave theory is a very powerful technique for analyzing unsteady flows and transient response. As applied to the stratified-to-slug flow regime transition, the method involves the velocities of:

- *continuity waves* which represent a relationship between flow rates and phase fractions, determined by an equilibrium of forces such as shear stress; and
- *dynamic waves* that depend upon restoring forces, such as gravity, which accelerate material through the wave as a result of phase fraction gradients.

The starting point of the one-dimensional wave theory is to perform a perturbation analysis on the unsteady, separated flow equations (modeling the stratified flow regime) and then to study the propagation of dynamic and continuity waves in the flow. The flow regime transition is assumed to occur when the criterion for a flow instability is satisfied. The transition from stratified to slug flow occurs when the squares of the dynamic and continuity wave velocities (c^2 and v_w^2) are equal in the model (see section 3).

Chapter 6 of the textbook by Wallis (1969) presents the derivation of the basic equations. That mathematical exercise is not repeated in this paper. This paper first focuses on the practical solution of the equations and the effectiveness of the model in predicting observed trends for a wide range of data.

Various authors, including Ferschneider *et al.* (1985), Lin & Hanratty (1986) and Wu *et al.* (1987), have presented models extending the one-dimensional wave model method. The problem has been approached at several levels. From the most complex to the simplest, these approaches range from:

- compressible flow of the vapor phase; to
- incompressible flow of both phases; to
- simplified, incompressible flow of both phases (without friction, but incorporating empirical coefficients).

Compressible flow model

Wallis (1969) has derived the basic equations for the case with compressible flow. This general model can be simplified for the purpose here, as described below.

Incompressible flow model

Wu *et al.* (1987) and Ferschneider *et al.* (1985) show that the effects of compressibility can be satisfactorily neglected in the model for the transport velocities of interest to pipelines, which simplifies the solution considerably. [See Wallis (1969, p. 149) for the development of the basic equations.] Wu *et al.* (1987) showed good comparisons with the regime transition data from Taitel & Dukler (1976) and their own experiments in the Shell KSLA facility at Bacton, England. Using an equivalent approach, but a somewhat different formulation of the model, Ferschneider *et al.* (1985) showed good comparisons over a range of pipe inclinations with flow regime data from a test facility located in Boussens, France.

The approach and basic equations of Wu *et al.* (1987) for incompressible gas–liquid flow in a pipe are used here. This paper provides mathematical details for closure and the solution methodology left to the reader in the previous work, so that the flow regime transition can be calculated using the equations presented here.

Incompressible flow model without friction

The mechanistic analysis proposed by Taitel & Dukler (1976) is widely used for the prediction of this flow regime transition. As first pointed out by Ferschneider *et al.* (1985), the basic Taitel–Dukler model is actually an approximation to the more general one-dimensional wave analysis. The key assumption is to omit friction in the momentum equations, which generally lowers the threshold for the instability. An empirical coefficient, which works best for flow conditions close to the original data, is then applied to the result. The simpler Taitel–Dukler model is usually adequate for determining the flow regime for pipeline calculations, as long as a factor of approximately 2 of uncertainty in the flow rates at the transition does not affect the predicted flow regime. The correspondence between the one-dimensional wave model presented here and the simplified Taitel–Dukler model is demonstrated further after the equations are presented.

The equations of the one-dimensional wave model (including the effects of friction) are presented first, followed by comparisons with a wide range of experimental data. The advantage of the more detailed mechanistic model is improved accuracy in predicting the flow regime transition at high gas density and at low gas velocity. The disadvantage is that the model is more complex to implement, and its numerical stability under all conditions has not been rigorously demonstrated.

As with any model, this model has limitations. It deals with the stratified-to-slug transition and is less effective for the slug-to-annular transition where the mechanism of the regime change is different—blow-through of the gas in the liquid slug. This wave theory is one-dimensional, predicts waves growing without limit and fits experimental data. There may be other phenomena to be considered if the liquid level is very low, e.g. Jepson *et al.* (1989).

When the equations are written in transient form, they can also be used not only to predict instability, but also to analyze how the interface will evolve as waves grow. This is an important feature of any theory that is to have the potential of predicting slug formation. This paper presents examples of waves growing and decaying by this mechanism.

Stratified flows that are unstable are usually also supercritical. This implies that both sets of dynamic waves propagate downstream and wash out any disturbances. Thus, cyclic slug formation is only possible if there is some other mechanism, perhaps associated with the inlet, to initiate disturbances at a fixed location.

2. BASIC EQUATIONS FOR STRATIFIED FLOW

The basic equations to be solved describe the conservation of mass and momentum for one-dimensional stratified motion in the x-direction, along the axis of the pipe. Compressibility effects are not included because they give rise to waves of an acoustic nature that travel much more rapidly (with speeds of the order of the speed of sound in each phase) than the interfacial waves that we will describe. This allows the phases to be treated as essentially incompressible and of a uniform density.

The one-dimensional transient equations of mass and momentum conservation for the gas phase illustrated in figure 1 are

$$\frac{\partial h}{\partial t} + U_G \frac{\partial h}{\partial x} - \frac{A_G}{A_L'} \frac{\partial U_G}{\partial x} = 0 \qquad [1]$$

and

$$\rho_G \left(\frac{\partial U_G}{\partial t} + U_G \frac{\partial U_G}{\partial x} + g \cos\theta \frac{\partial h}{\partial x} \right) = -\frac{\partial P}{\partial x} - \frac{\tau_{WG} S_G}{A_G} - \frac{\tau_i S_i}{A_G} - g\rho_G \sin\theta. \qquad [2]$$

The nomenclature is the same as that adopted by Taitel & Dukler (1977). P is the interface pressure and

$$A_L' = \frac{dA_L}{dh} = S_i, \qquad [3]$$

which is the width of the interface between the gas and the liquid. The cross-sectional areas of the phases (A_L and A_G), as well as the perimeter of the phases on the wall and at the interface (S_L, S_G and S_i), are all functions of "h" and the particular geometry of the pipe, which we will assume to be circular in cross section; θ is the inclination of the pipe from the horizontal.

The corresponding equations for the liquid are

$$\frac{\partial h}{\partial t} + U_L \frac{\partial h}{\partial x} + \frac{A_L}{A_L'} \frac{\partial U_L}{\partial x} = 0 \qquad [4]$$

and

$$\rho_L \left(\frac{\partial U_L}{\partial t} + U_L \frac{\partial U_L}{\partial x} + g \cos\theta \frac{\partial h}{\partial x} \right) = -\frac{\partial P}{\partial x} - \frac{\tau_{WL} S_L}{A_L} + \frac{\tau_i S_i}{A_L} - g\rho_L \sin\theta. \qquad [5]$$

Equilibrium solution

The steady-state equilibrium solution for holdup in a stratified flow is obtained by equating all the differentials in [2] and [5] to zero and eliminating P. The result is a single equation which can

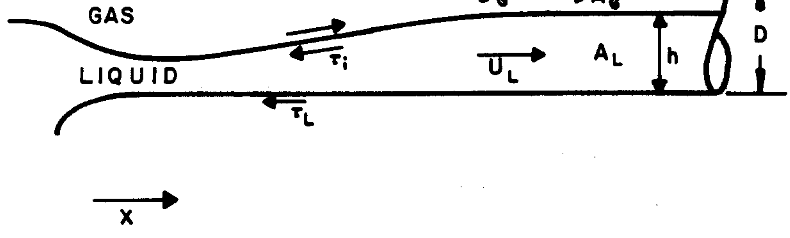

Figure 1. Nomenclature for gas–liquid stratified flow.

be solved for the liquid level or holdup, if the shear stresses are expressed in terms of known friction factors:

$$F = \frac{f_{WL}\rho_L\left(\frac{\pi}{4}\right)^2 \tilde{S}_L U_{LS}^2}{2D\tilde{A}_L^3} - \frac{f_{WG}\rho_G\left(\frac{\pi}{4}\right)^2 \tilde{S}_G U_{GS}^2}{2D\tilde{A}_G^3}$$

$$\mp \frac{f_i\rho_G\left(\frac{\pi}{4}\right)^3 \tilde{S}_i}{2D}\left(\frac{U_{GS}^2}{\tilde{A}_L\tilde{A}_G^3} - \frac{2U_{LS}U_{GS}}{\tilde{A}_L^2\tilde{A}_G^2} + \frac{U_{LS}^2}{\tilde{A}_L^3\tilde{A}_G}\right) + g(\rho_L - \rho_G)(\sin\theta) = 0. \quad [6]$$

The terms in this equation are functions of the liquid level (or liquid fraction) and the superficial phase velocities (U_{LS} and U_{GS}). The sign on the third term is negative if $U_G > U_L$ and positive if $U_L > U_G$. The dimensionless geometric parameters in [6] are also functions of the liquid level:

$$\tilde{A}_L = \frac{A_L}{D^2} = \tfrac{1}{4}\{\pi - \cos^{-1}(2h^* - 1) + (2h^* - 1)[1 - (2h^* - 1)^2]^{0.5}\}, \quad [7]$$

$$\tilde{A}_G = \frac{A_G}{D^2} = \tfrac{1}{4}\{\cos^{-1}(2h^* - 1) - (2h^* - 1)[1 - (2h^* - 1)^2]^{0.5}\}, \quad [8]$$

$$\tilde{S}_L = \frac{S_L}{D} = [\pi - \cos^{-1}(2h^* - 1)], \quad [9]$$

$$\tilde{S}_G = \frac{S_G}{D} = [\cos^{-1}(2h^* - 1)] \quad [10]$$

and

$$\tilde{S}_i = \frac{S_i}{D} = [1 - (2h^* - 1)^2]^{0.5}, \quad [11]$$

where h^* is the dimensionless liquid level (h/D). $\tilde{A}_L$ and $\tilde{A}_G$ are the dimensionless cross-sectional areas of the pipe occupied by the liquid and gas phases. $\tilde{S}_L$, $\tilde{S}_G$ and $\tilde{S}_i$ are the dimensionless perimeters of the wall–liquid interface, gas–wall interface and gas–liquid interface, respectively.

Equation [6] incorporates the shear relationships as follows:

$$\tau_{WL} = \frac{f_{WL}\rho_L U_L^2}{2}, \quad [12]$$

if the liquid flow is restricted to positive values (no counter flow),

$$\tau_{WG} = \frac{f_{WG}\rho_G U_G^2}{2} \quad [13]$$

and

$$\tau_i = \frac{f_i\rho_G(U_G - U_L)|(U_G - U_L)|}{2}, \quad [14]$$

where τ_{WL}, τ_{WG} and τ_i are the shear stresses at the wall–liquid, wall–gas and gas–liquid interfaces, respectively. Note that the velocity difference ($U_G - U_L$) is used in the interfacial shear term in [14]. Sometimes U_G can simply be used, neglecting the liquid velocity if $U_G \gg U_L$. Since the flow regime transition is not very sensitive to the selection of the friction factors, constant friction factors have been used in [6], e.g.

$$f_{WL} = f_{WG} = f_i = 0.005.$$

Continuity wave velocity

In order to use the stability criterion developed in Wallis (1969), we need expressions for the continuity and dynamic wave velocities. The former may be derived directly from the equilibrium condition [6] and is expressed as the difference between the wave velocity and a relative velocity:

$$v_{\rm w} = (V_{\rm w} - V_0). \tag{15}$$

The reference velocity V_0 (Wallis 1969) is

$$V_0 = \frac{\left(\frac{\pi}{4}\right)\left(\frac{\rho_{\rm L} U_{\rm LS}}{\tilde{A}_{\rm L}^2} + \frac{\rho_{\rm G} U_{\rm GS}}{\tilde{A}_{\rm G}^2}\right)}{\left(\frac{\rho_{\rm L}}{\tilde{A}_{\rm L}} + \frac{\rho_{\rm G}}{\tilde{A}_{\rm G}}\right)}. \tag{16}$$

For most cases, this weighted mean velocity has a numerical value which is close to the actual liquid velocity $U_{\rm L}$.

The general relationship used to derive the wave velocity $V_{\rm w}$ is

$$V_{\rm w} = \left(\frac{\partial U_{\rm LS}}{\partial \epsilon_{\rm L}}\right)_{(U_{\rm LS}+U_{\rm GS})} = \frac{-\left(\frac{\partial F}{\partial \tilde{A}_{\rm L}}\right)\left(\frac{\pi}{4}\right)}{\left(\frac{\partial F}{\partial U_{\rm LS}}\right) - \left(\frac{\partial F}{\partial U_{\rm GS}}\right)}. \tag{17}$$

Wallis (1969) presents the general derivative as a function of liquid fraction, and Wu *et al.* (1987) derive the expanded version of the derivative in terms of the superficial velocities. In this equation, the derivatives of the function F in [6] are defined as follows:

$\left(\frac{\partial F}{\partial \tilde{A}_{\rm L}}\right)$ is the partial derivative of F with respect to $\tilde{A}_{\rm L}$ with the superficial gas velocity $U_{\rm GS}$ and the superficial liquid velocity $U_{\rm LS}$ constant.

$\left(\frac{\partial F}{\partial U_{\rm LS}}\right)$ is the partial derivative of F with respect to the superficial liquid velocity when the liquid level and the superficial gas velocity $U_{\rm GS}$ are constant.

$\left(\frac{\partial F}{\partial U_{\rm GS}}\right)$ is the partial derivative of F with respect to the superficial gas velocity when the liquid level and the superficial liquid velocity $U_{\rm LS}$ are constant.

These derivatives can be calculated either numerically or explicitly.

Numerical approach. The numerical approach is to evaluate the derivatives by perturbing $\tilde{A}_{\rm L}$ (or h^*), $U_{\rm LS}$ or $U_{\rm GS}$ by a small amount (say $\pm 1\%$) in [6]. This approach has the advantage of allowing variable friction factors to be used in the model (see section 2).

Explicit derivatives. Explicit equations for these derivatives have been obtained by differentiating [6] (with constant friction factors) to obtain:

$$\left(\frac{\partial F}{\partial U_{\rm LS}}\right) = \left[\frac{f_{\rm WL}\rho_{\rm L}\left(\frac{\pi}{4}\right)^2 \tilde{S}_{\rm L}\tilde{A}_{\rm L}^{-3} U_{\rm LS}}{D}\right]$$

$$\pm \left[\frac{f_{\rm i}\rho_{\rm G}\left(\frac{\pi}{4}\right)^3 \tilde{S}_{\rm i}\tilde{A}_{\rm L}^{-1}\tilde{A}_{\rm G}^{-1}}{D}\right](-U_{\rm LS}\tilde{A}_{\rm L}^{-2} + U_{\rm GS}\tilde{A}_{\rm L}^{-1}\tilde{A}_{\rm G}^{-1}), \tag{18}$$

$$\left(\frac{\partial F}{\partial U_{\rm GS}}\right) = -\left[\frac{f_{\rm WG}\rho_{\rm G}\left(\frac{\pi}{4}\right)^2 \tilde{S}_{\rm G}\tilde{A}_{\rm G}^{-3} U_{\rm GS}}{D}\right]$$

$$\mp \left[\frac{f_{\rm i}\rho_{\rm G}\left(\frac{\pi}{4}\right)^3 \tilde{S}_{\rm i}\tilde{A}_{\rm L}^{-1}\tilde{A}_{\rm G}^{-1}}{D}\right](-U_{\rm LS}\tilde{A}_{\rm L}^{-1}\tilde{A}_{\rm G}^{-1} + U_{\rm GS}\tilde{A}_{\rm G}^{-2}) \tag{19}$$

and

$$\left(\frac{\partial F}{\partial \tilde{A}_L}\right) = \left[\frac{f_{WL}\rho_L\left(\frac{\pi}{4}\right)^2 U_{LS}^2}{2D}\right]\left[\tilde{A}_L^{-3}\left(\frac{\partial \tilde{S}_L}{\partial \tilde{A}_L}\right) - 3\tilde{S}_L\tilde{A}_L^{-4}\right]$$
$$- \left[\frac{f_{WG}\rho_G\left(\frac{\pi}{4}\right)^2 U_{GS}^2}{2D}\right]\left[\tilde{A}_G^{-3}\left(\frac{\partial \tilde{S}_G}{\partial \tilde{A}_L}\right) + 3\tilde{S}_G\tilde{A}_G^{-4}\right]$$
$$\mp \left[\frac{f_i\rho_G\left(\frac{\pi}{4}\right)^3}{2D}\right]\left\{U_{GS}^2\left[\tilde{A}_L^{-1}\tilde{A}_G^{-3}\left(\frac{\partial \tilde{S}_i}{\partial \tilde{A}_L}\right) - \tilde{S}_i\tilde{A}_L^{-2}\tilde{A}_G^{-3} + 3\tilde{S}_i\tilde{A}_L^{-1}\tilde{A}_G^{-4}\right]\right.$$
$$- 2U_{LS}U_{GS}\left[\tilde{A}_L^{-2}\tilde{A}_G^{-2}\left(\frac{\partial \tilde{S}_i}{\partial \tilde{A}_L}\right) - 2\tilde{S}_i\tilde{A}_L^{-3}\tilde{A}_G^{-2} + 2\tilde{S}_i\tilde{A}_L^{-2}\tilde{A}_G^{-3}\right]$$
$$\left. + U_{LS}^2\left[\tilde{A}_L^{-3}\tilde{A}_G^{-1}\left(\frac{\partial \tilde{S}_i}{\partial \tilde{A}_L}\right) - 3\tilde{S}_i\tilde{A}_L^{-4}\tilde{A}_G^{-1} + \tilde{S}_i\tilde{A}_L^{-3}\tilde{A}_G^{-2}\right]\right\}. \qquad [20]$$

These explicit derivatives are only valid if constant friction factors are assumed. Use the upper sign in each if $U_G > U_L$ and the lower sign if $U_L > U_G$ (as in [6]). Equation [20] requires additional geometric parameters, defined by

$$\left(\frac{\partial \tilde{S}_L}{\partial \tilde{A}_L}\right) = \frac{2}{[1-(2h^*-1)^2]}, \qquad [21]$$

$$\left(\frac{\partial \tilde{S}_G}{\partial \tilde{A}_L}\right) = -\left(\frac{\partial \tilde{S}_L}{\partial \tilde{A}_L}\right) = -\frac{2}{[1-(2h^*-1)^2]} \qquad [22]$$

and

$$\left(\frac{\partial \tilde{S}_i}{\partial \tilde{A}_L}\right) = -\frac{2(2h^*-1)}{[1-(2h^*-1)^2]}. \qquad [23]$$

Dynamic wave velocity

If $\mathrm{d}P/\mathrm{d}x$ is eliminated from [2] and [5], [1] and [4] may be used to show that the "characteristics" of the equation set represent "dynamic waves" (Wallis 1969) traveling at speeds $V_0 \pm c$, where

$$c^2 = \frac{\dfrac{gD(\rho_L-\rho_G)(\cos\theta)}{\tilde{S}_i} - \dfrac{\left(\frac{\pi}{4}\right)^2\left(\frac{U_{GS}}{\tilde{A}_G} - \frac{U_{LS}}{\tilde{A}_L}\right)^2}{\left(\frac{\tilde{A}_L}{\rho_L} + \frac{\tilde{A}_G}{\rho_G}\right)}}{\left(\dfrac{\rho_L}{\tilde{A}_L} + \dfrac{\rho_G}{\tilde{A}_G}\right)}. \qquad [24]$$

This is the form used in the solution presented in this paper. For reference, the correspondence of this relationship with the Taitel–Dukler (1976) analysis is discussed here. As shown by Wu *et al.* (1987), the Taitel–Dukler (1976) analysis is equivalent to setting $c^2 = 0$ in [24] to obtain

$$\mathrm{Fr}_G = \left[\frac{\rho_G}{\Delta\rho g D(\cos\theta)}\right]^{0.5}\left(\frac{U_{GS}}{\tilde{A}_G} - \frac{U_{LS}}{\tilde{A}_L}\right) = \frac{4}{\pi}\left[\tilde{A}_G^3\left(1 + \frac{\rho_G\tilde{A}_L}{\rho_L\tilde{A}_G}\right)\tilde{S}_i^{-1}\right]^{0.5}. \qquad [25]$$

With the additional assumptions made by Taitel & Dukler (1976) that

$$\rho_G \ll \rho_L$$

and

$$U_G \gg U_L,$$

[25] simplifies further to

$$\mathrm{Fr}_G = \left(\frac{\rho_G U_{GS}^2}{\Delta\rho g D(\cos\theta)}\right)^{0.5} = \frac{4}{\pi}\left(\tilde{A}_G \tilde{S}_i^{-1}\right)^{0.5}, \qquad [26]$$

which is identical to the transition criterion for a critical gas velocity proposed by Taitel & Dukler (1976), if the empirical coefficient $(1 - h^*)$ multiplies the right-hand side. For flow in rectangular channels, Wallis & Dobson (1973) suggested a coefficient of about 0.5, which is similar to what Kordyban & Ranov (1970) obtained.

3. TRANSITION CRITERION

In the Taitel–Dukler (1976) approach, [26] can be solved directly for the critical gas velocity at an assumed liquid level h^*, i.e. there is no dependence on the liquid velocity U_{GL}. Then [6] can be solved to obtain the corresponding liquid velocity. The flow regime transition can be mapped by assuming various liquid levels (in the range $0 < h^* < 1$) in order to obtain the (U_{GS}, U_{LS}) pairs which map the flow regime transition.

An alternative approach, which is consistent with the more complete one-dimensional analysis presented here, is based on the criterion that instability results when the continuity waves overtake dynamic waves (Wallis 1969); we call this the "one-dimensional wave model".

Since dynamic waves move with a velocity of $\pm c$ relative to the weighted mean velocity V_0, while continuity waves move only in one direction at the velocity v_w, the criterion for instability involves the squares of the velocities:

$$v_w^2 > c^2. \qquad [27]$$

The stratified-to-slug flow regime transition occurs when the two velocities are equal in [27]. Since v_w and c depend upon the liquid fraction and both superficial phase velocities, by [15]–[17] and [24] it is not possible to solve explicitly for one parameter in terms of the other two parameters. Therefore, an iterative solution procedure is required to find the flow regime transition.

The iterative procedure to find the flow regime transition by this model is as follows:

(1) Use the given value of U_{GS} for the flow conditions in the pipe and guess a value of the liquid level h^* between 0 and 1. For example, start with $h^* = 0.5$.
(2) Evaluate the geometric parameters ([7]–[11] and [21]–[23]).
(3) Solve [6] for the superficial liquid velocity U_{LS} at equilibrium conditions, i.e. $F = 0$. Equation [6] can be solved explicitly if constant friction factors are assumed; otherwise, an iterative solution should be used. Check if $U_G > U_L$. If $U_G > U_L$, then use upper sign in [6], if not use the lower sign.
(4) Calculate the dynamic wave velocity c^2 from [24].
(5) Calculate the continuity wave velocity v_w^2 using [15]–[17]. Equations [18]–[20] may be used to evaluate [17]. If $U_G > U_L$ (see Step 3) then use the upper sign, if not use the lower.
(6) Iterate on the guessed value of h^* until the squares of the two velocities match. Generally, the relationship $v_w^2 < c^2$ will be true if the value of h^* is too low, and the converse will be true ($v_w^2 > c^2$) if the value of h^* is too high.

Although this solution procedure has been implemented and checked out for many cases, the existence of a solution for all possible conditions has not been rigorously proved.

Sample calculations

Figure 2 compares the one-dimensional wave model (——) with the original Taitel–Dukler (1976) analysis (– – –). The conditions for these comparisons and data are the same as for the data upon which the Taitel–Dukler analysis is based, namely small-diameter (0.025 m) horizontal pipes with flowing air and water at near-atmospheric pressure (Barnea *et al.* 1980). The smooth-pipe correlations for friction factors have been used as recommended in the original model for the Taitel–Dukler analysis. As noted in section 2, constant friction factors are used in the

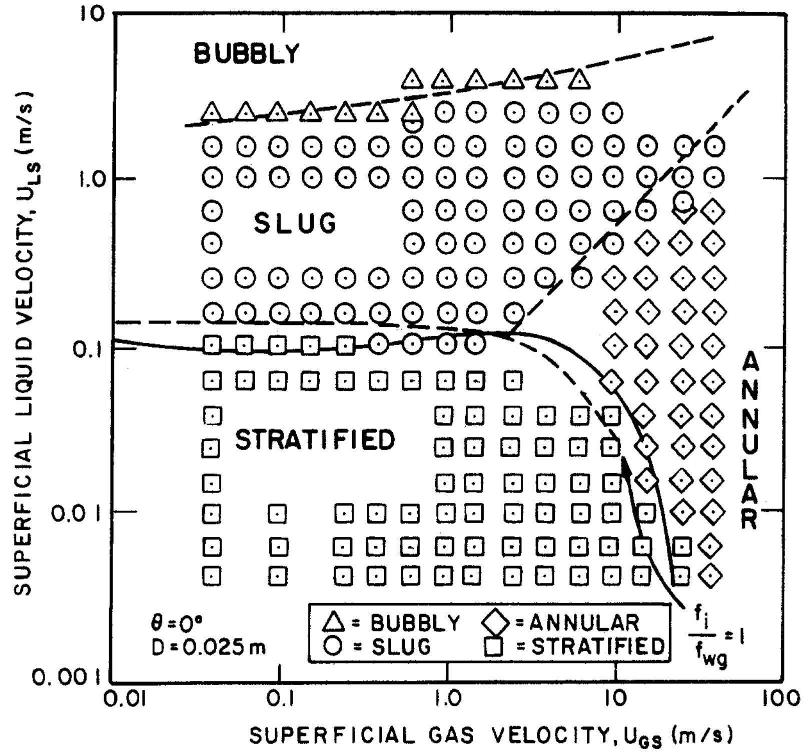

Figure 2. Stratified transition for a horizontal 0.025 m dia pipe at low gas density (Barnea et al. 1980). ——, One-dimensional wave model; ---, Taitel–Dukler (1976) model.

one-dimensional wave model. This figure shows that there are only small differences in the predicted stratified-to-slug transition between the two modeling approaches for these conditions.

The equation for the continuity wave velocity [17] has been solved both explicitly (by using derivatives of the steady-state equations in [18]–[20]) and also numerically. The numerical result was obtained by evaluating the variation in the function F for $\pm 1\%$ variations in the values of the parameters in the derivatives. The results via either approach are negligibly different.

Figure 3 illustrates example solutions using the one-dimensional wave model. In figure 3, both the continuity and dynamic wave velocities are plotted as a function of the superficial liquid velocity at various constant values of the superficial gas velocity. The continuity wave velocity (---) monotonically increases with increasing superficial liquid velocity, and the wave velocity is greater for greater superficial gas velocity. The dynamic wave velocity (——) may have two values in each case. The intersection of the dashed and solid lines for the same gas velocity defines the superficial liquid velocity for the solution and hence the locus of the transition as (U_{GS}, U_{LS}) pairs.

4. COMPARISONS WITH FLOW REGIME TRANSITION DATA

Flow regime data have been obtained by various investigators over a wide range of test conditions. Table 1 summarizes the conditions of the experiments for which comprehensive comparisons with the predictions of the one-dimensional wave model have been made. Selected comparisons are presented here in order to illustrate the parametric effects of pipe diameter, gas density and pipe inclination.

Low gas density

Figures 2–6 illustrate the effect of pipe diameters from 0.0254 to 0.30 m for common test conditions of:

- air and water;
- horizontal pipes; and
- near-atmospheric pressure.

Table 1. Conditions for experiments in various test facilities

Facility	Pipe i.d. (m)	Length L/D	Inclination (°)	Pressure (bar)	Liquid density (kg/m^3)	Gas density (kg/m^3)	Density ratio ρ_L/ρ_G	Surface tension (kg/m)	Liquid viscosity (kg/m-s)	$a = \left[\frac{gD(\rho_L-\rho_G)}{\rho_L}\right]^{1/2}$ (m/s)	$b = \left[\frac{gD(\rho_L-\rho_G)}{\rho_G}\right]^{1/2}$ (m/s)	Reference
Creare/PRC	0.089	400	−2, 0, 2	5.4	995	32.1	31	0.070	1×10^{-3}	0.91	5.12	Crowley *et al.* (1988)
	0.17	200	0	5.4	995	32.1	31	0.070	1×10^{-3}	1.28	7.10	Crowley & Sam (1986)
IFP (Boussens)	0.146	822	−0.057, 0, 4	15	710	14.4	49	0.020	0.35×10^{-3}	1.19	8.29	Bendiksen *et al.* (1986)
SINTEF (Trondheim)	0.189	2000	0	30	890	32.1	28	0.022	2×10^{-3}	1.34	7.04	Ferschneider *et al.* (1985)
Univ. of Strathclyde	0.13	123	0	1	995	≅1.2	≅830	0.076	1×10^{-3}	1.12	32.5	Simpson (1981)
	0.22	73		1	995	≅1.9	≅830	0.076	1×10^{-3}	1.46	42.2	
Harwell	0.30	200	0	1.0 to 1.8	995	≅1.2	≅830	0.076	1×10^{-3}	1.71	49.4	Jepson *et al.* (1989)
	0.15	230		1	995	≅1.2	≅830	0.076	1×10^{-3}	1.21	34.9	Kouba & Jepson (1989)
Tel-Aviv Univ.	0.025	394	−90 to +90	1	995	≅1.2	≅830	0.076	1×10^{-3}	0.49	14.3	Barnea *et al.* (1980, 1982)
	0.051	146		1	995	≅1.2	≅830	0.076	1×10^{-3}	0.71	20.4	

$Fr_G = U_{GS}/b$, $Fr_L = U_{LS}/a$.

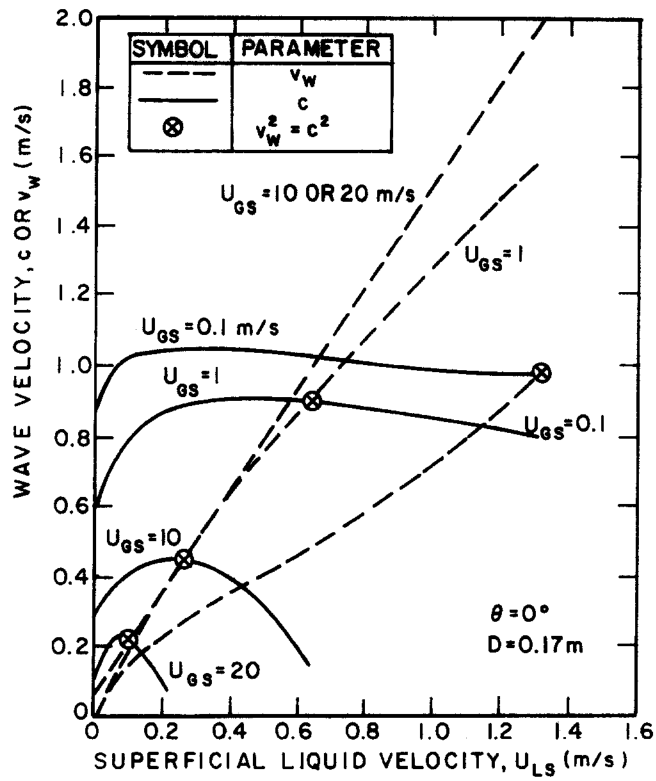

Figure 3. Illustration of wave velocity calculations for the one-dimensional model.

For the bulk of the flow regime data, especially at $U_{GS} > 0.1$ m/s, the predictions of the stratified-to-slug regime transition with the one-dimensional wave model are within a factor of 2 of the observed liquid velocities, even for a very large pipe diameter of 0.3 m (figure 6), where the transition tends to be underpredicted by about that much. The calculated transitions also lie in close agreement with the Taitel–Dukler (1976) analysis.

Figure 5 is particularly interesting because of the transition behavior observed at very low gas velocity ($U_{GS} < 0.1$ m/s). The transition appears to occur at higher liquid velocity, giving a concave appearance to the transition locus. The one-dimensional wave model predicts this trend. This trend is not predicted by the simpler Taitel–Dukler analysis. As shown below, this trend becomes more pronounced at higher gas density.

Wu *et al.* (1987) demonstrated that the location of the "cusp" (concave feature) in the calculations can be changed if different assumptions are made about the interfacial friction. [Compare the Wu *et al.* (1987) predictions for $f_i = 0.005$ and $\varepsilon_i = \varepsilon_w$ in figure 1 of that reference. The parameters ε_i and ε_w are the roughness of the interface and the wall, respectively.] Thus, additional tuning of the model could improve the comparisons at low velocity.

High gas density

Figures 7–10 compare the predicted and experimental transitions for data in horizontal pipes at high gas density. Figures 7 and 8 are for the Creare/PRC 0.089 and 0.17 m dia pipes (Crowley & Sam 1986; Crowley *et al.* 1988), figure 9 is for the SINTEF 0.20 m pipe (Bendiksen *et al.* 1986) and figure 10 is for the Boussens 0.15 m pipe (Ferschneider *et al.* 1985). In these facilities the gas density is 15–30 kg/m^3, or about 15–30 times the density of air at atmospheric pressure. The various test fluids, including hydrocarbons, water and Freon are noted in table 1.

Once again, the trend in the data at low gas velocities compares well with the Creare/PRC data for 0.09 and 0.17 m pipe sizes in figures 7 and 8. The SINTEF and Boussens data (figures 9 and 10) do not extend to such low gas velocities as in the Creare/PRC tests. Those data lie in the range where the one-dimensional wave model and the Taitel–Dukler (1976) analysis both lie in close agreement with the data. The divergence of the data from the Taitel–Dukler analysis at low gas

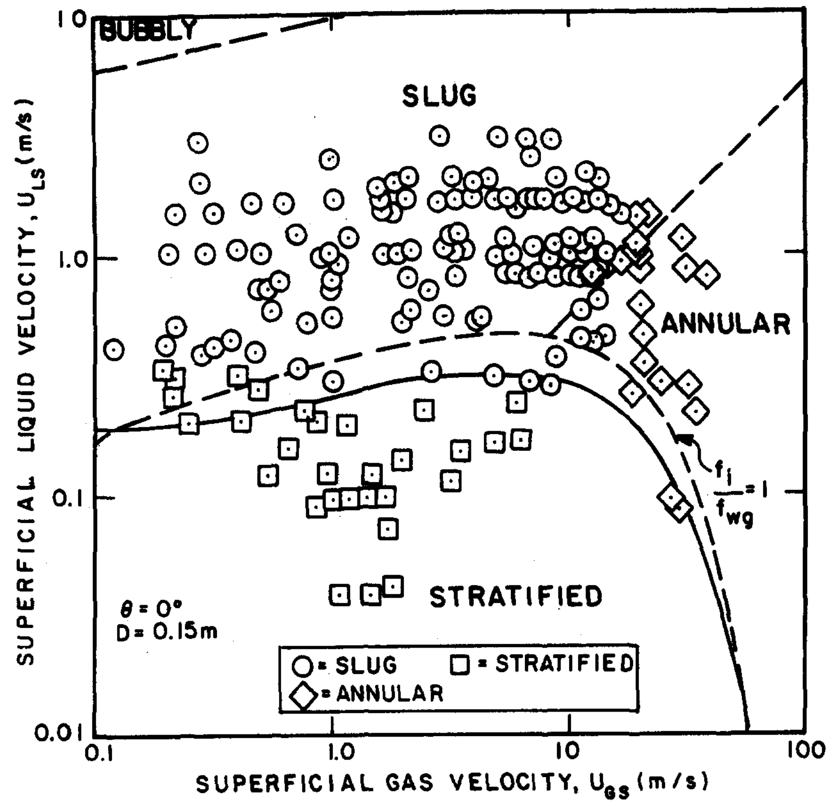

Figure 4. Stratified transition for a horizontal 0.15 m dia pipe at low gas density (Kouba & Jepson 1989). ——, One-dimensional wave model; – – –, Taitel–Dukler (1976) model.

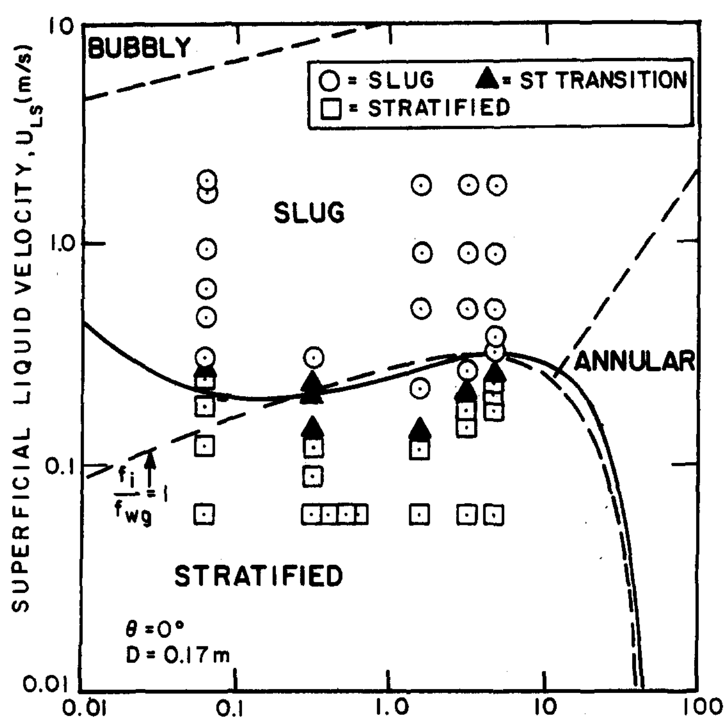

Figure 5. Stratified transition for a horizontal 0.17 m dia pipe at low gas density (Crowley & Sam 1986). ——, One-dimensional wave model; – – –, Taitel–Dukler (1976) model.

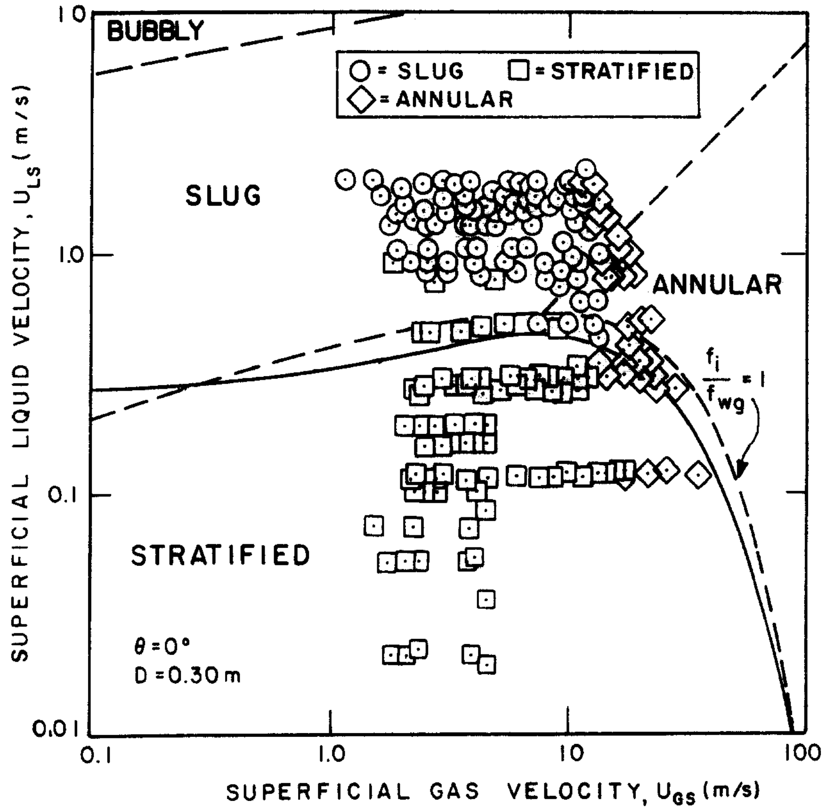

Figure 6. Stratified transition for a horizontal 0.30 m dia pipe at low gas density (Jepson et al. 1989). ——, One-dimensional wave model; ---, Taitel–Dukler (1976) model.

velocity is predicted well by the one-dimensional wave model presented here. This is the range where the assumption $U_G \gg U_L$ in the Taitel–Dukler model is no longer applicable.

It is interesting to note that the one-dimensional wave model presented here compares well with the data at both low and high gas density. See, for example, the comparisons in figures 5 and 8,

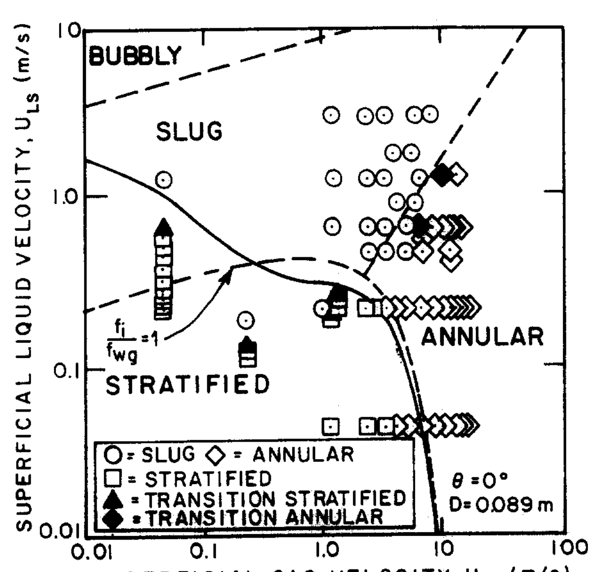

Figure 7. Stratified transition for a horizontal 0.089 m dia pipe at high gas density (Crowley et al. 1988). ——, One-dimensional wave model; ---, Taitel–Dukler model.

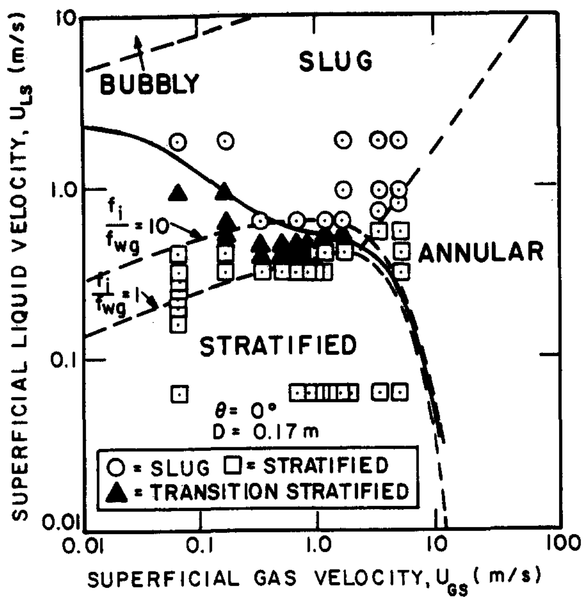

Figure 8. Stratified transition for a horizontal 0.17 m dia pipe at high gas density (Crowley & Sam 1986). ——, One-dimensional wave model; ---, Taitel–Dukler (1976) model.

which are in the same test facility. The one-dimensional wave model predicts the data at both gas densities.

The original Taitel–Dukler (1976) model, with its assumption of a smooth gas–liquid interface in [6] ($f_i = f_{wg}$ or $f_i/f_{wg} = 1$), compares less well at high gas density. This result has, in the past, led to the recommendation of increasing the interfacial shear in the model (Crowley & Sam, 1986). Figure 8 shows that a factor of 10 increase in the interfacial shear ($f_i = 10 f_{wg}$ or $f_i/f_{wg} = 10$) is

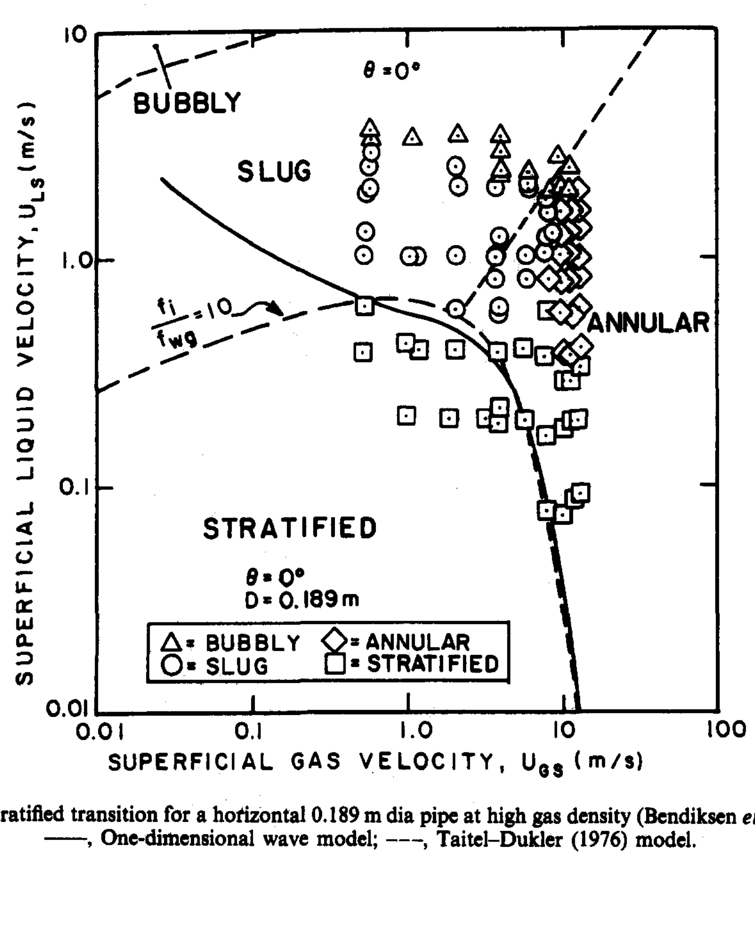

Figure 9. Stratified transition for a horizontal 0.189 m dia pipe at high gas density (Bendiksen *et al.* 1986). ——, One-dimensional wave model; ---, Taitel–Dukler (1976) model.

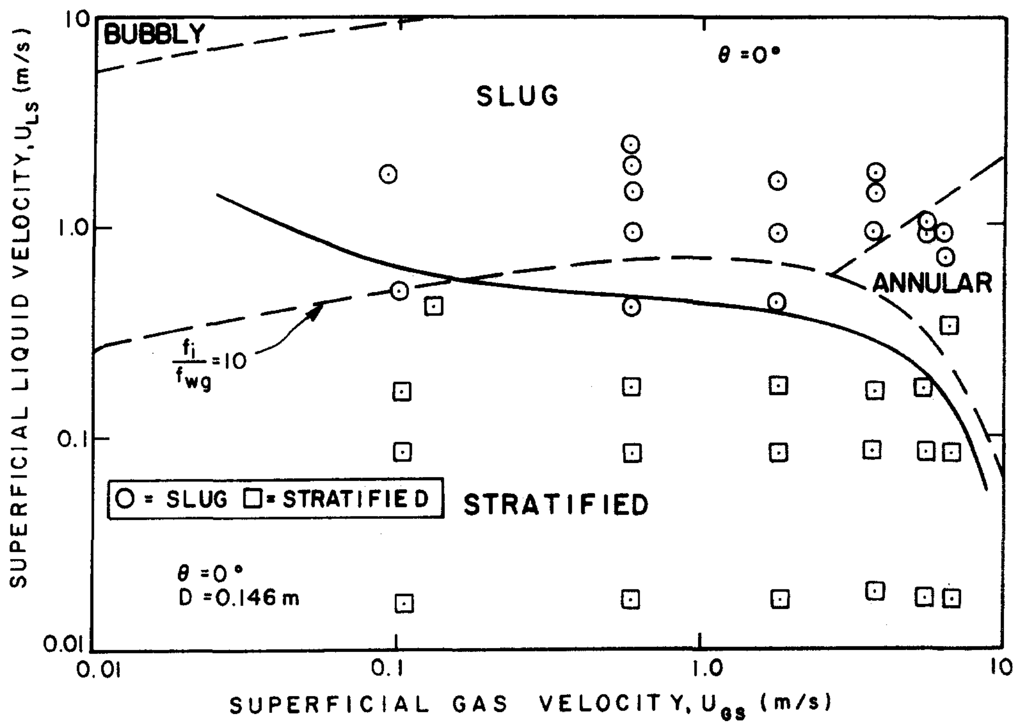

Figure 10. Stratified transition for a horizontal 0.146 m dia pipe at high gas density (Ferschneider *et al.* 1985). ——, One-dimensional wave model; ---, Taitel–Dukler (1976) model.

an improvement to the comparison at $U_{GS} > 0.1$ m/s, but does not fully match the trend in the data at lower gas velocity.

In all subsequent comparisons at high gas density the higher value of interfacial shear ($f_i/f_{wg} = 10$) is used in the Taitel–Dukler analysis. The original friction factors are used in the one-dimensional wave model.

Pipe inclination

Figures 11–13 compare the predicted and observed flow regime transitions for downwardly inclined pipes. Figure 11 is a comparison with data at low pressure in a small pipe inclined at $-1°$ (Barnea *et al.* 1982). Consistent with the comparisons for a horizontal pipe (figure 1), the predictions of the one-dimensional wave model are in close agreement with both the Taitel–Dukler (1976) analysis and the data. Figures 12 and 13 are for experimental data at high pressure in large pipes at inclinations of $-0.057°$ and $-2°$ (Ferschneider *et al.* 1985; Crowley & Sam 1986). The model presented here is satisfactory for these cases as well. Note that the concave feature of the transition which is observed with the horizontal pipes is absent in both the data and the predictions for downward inclinations.

Figure 14 presents a flow regime comparison for a pipe inclined upward at 1° (Barnea *et al.* 1980). This comparison is again for data at low gas density in a small pipe. Consistent with the results at other inclinations (figures 2 and 11), the predictions of the one-dimensional wave model at low pressure are similar to the Taitel–Dukler (1976) analysis. Figures 15 and 16 show comparisons with flow regime data in large pipes at upward inclinations of 2° (Crowley & Sam 1986) and 4° (Ferschneider *et al.* 1985) at high gas density. Figure 15 compares the model with the 2° upslope data in the Creare/PRC facility at 0.17 m dia. Figure 16 compares the data from the 0.15 m pipe at Boussens. The one-dimensional wave model tends to underpredict the size of the stratified region somewhat for the upsloping pipes; however, the results are not far from those of the Taitel–Dukler (1976) model.

The figures presented above demonstrate that the one-dimensional wave model provides comparisons which are generally comparable with the Taitel–Dukler (1976) model at low gas density, small pipe diameter and high gas velocity ($U_{GS} > 0.1$ m/s). For the cases of low gas

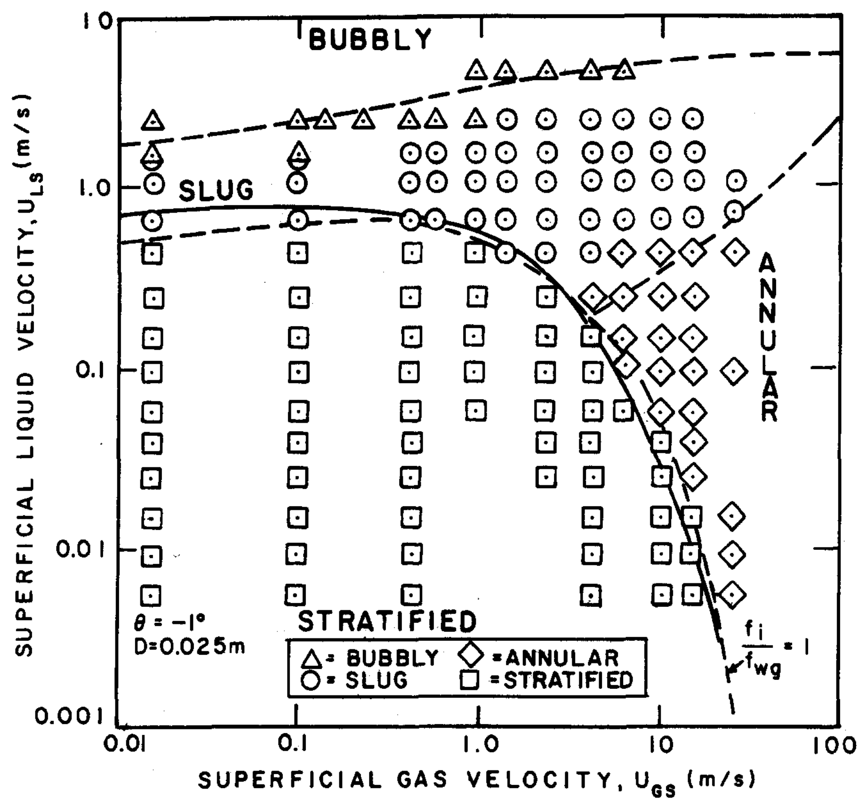

Figure 11. Stratified transition for a downward inclined (−1°) 0.025 m dia pipe (Barnea *et al.* 1982). ——, One-dimensional wave model; – – –, Taitel–Dukler (1976) model.

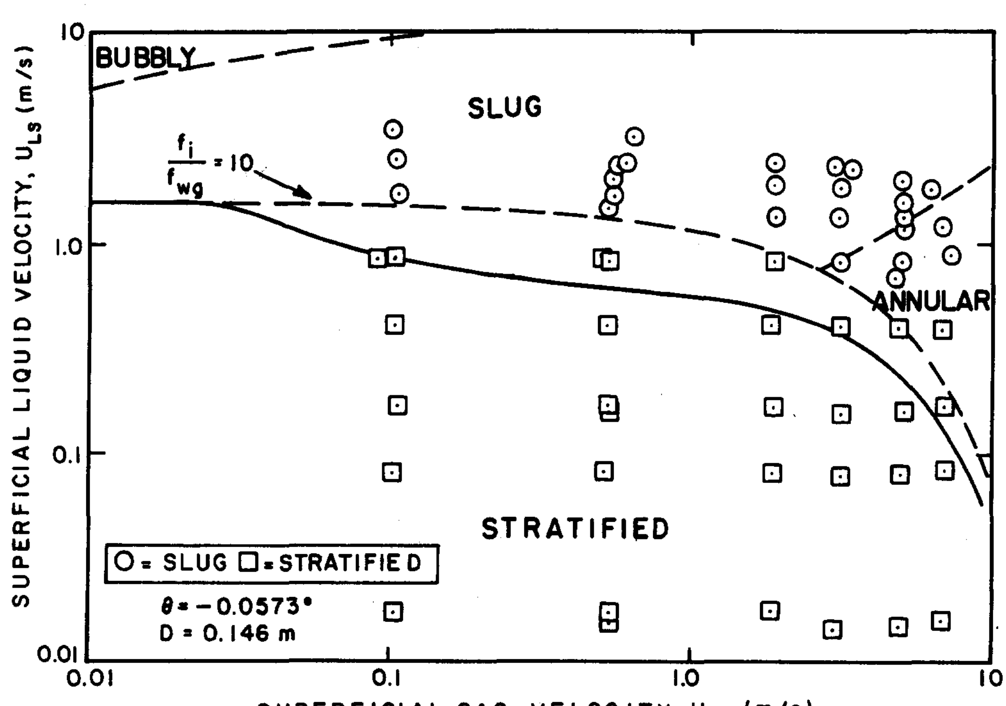

Figure 12. Stratified transition for a downward inclined (−0.057°) 0.146 m dia pipe (Ferschneider *et al.* 1985). ——, One dimensional wave model; – – –, Taitel–Dukler (1976) model.

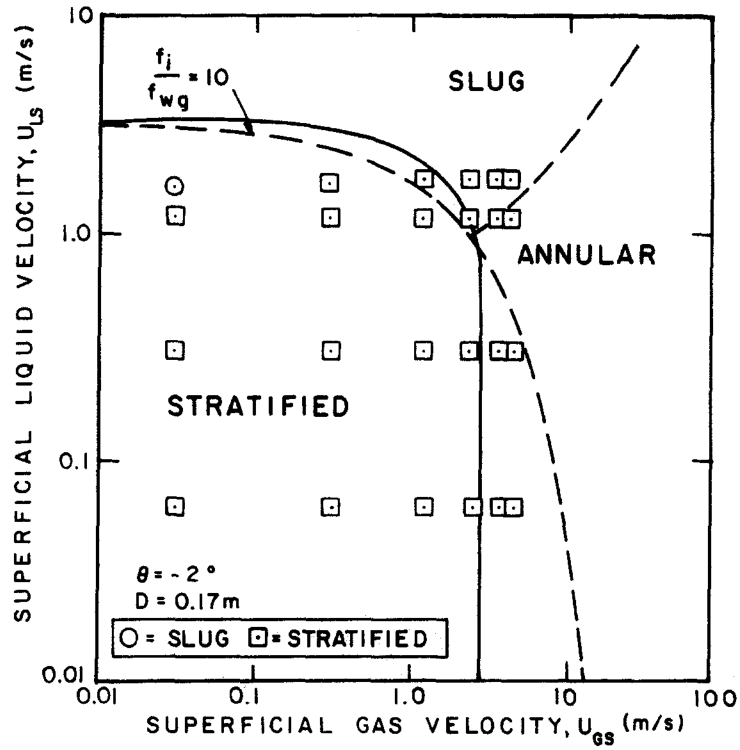

Figure 13. Stratified transition for a downward inclined (−2°) 0.17 m dia pipe (Crowley & Sam 1986). ——, One-dimensional wave model; ---, Taitel–Dukler (1976) model.

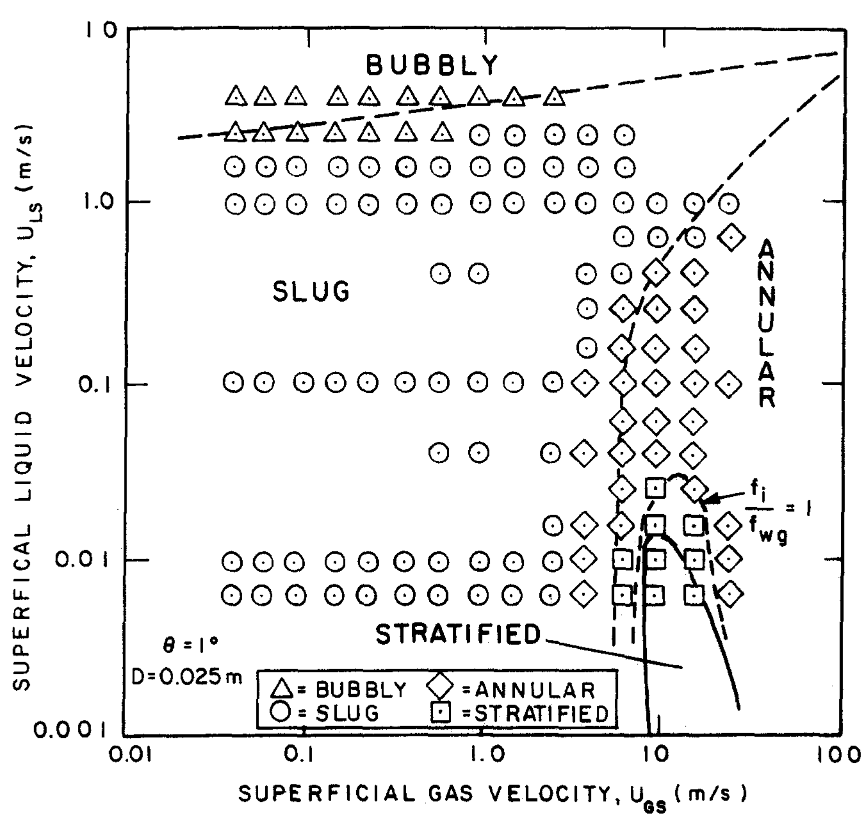

Figure 14. Stratified transition for an upward inclined (1°) 0.025 m dia pipe (Barnea et al. 1982). ——, One-dimensional wave model; ---; Taitel–Dukler model.

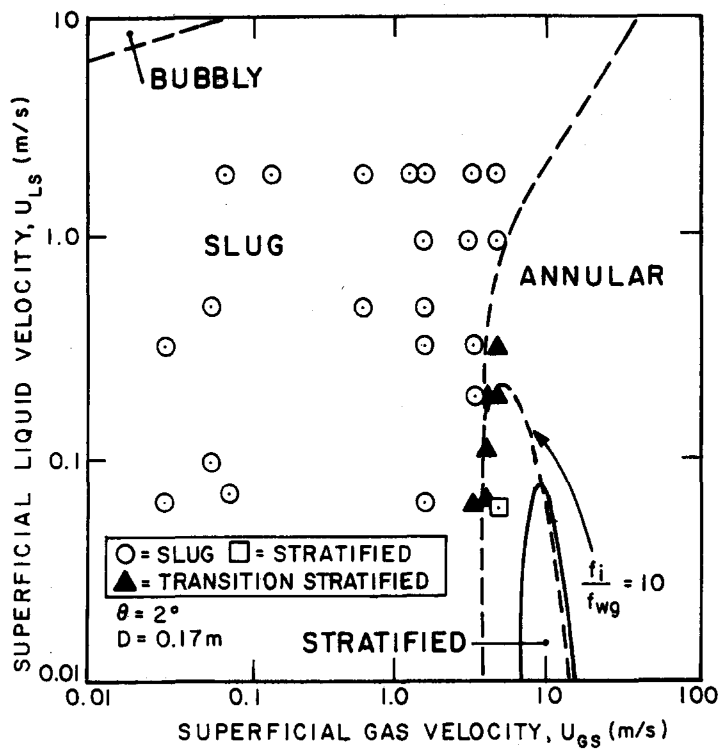

Figure 15. Stratified transition for an upward inclined (2°) 0.17 m dia pipe (Crowley & Sam 1986). ——, One-dimensional wave model; – – –, Taitel–Dukler (1976) model.

velocity and high gas density the model presented here is superior to the Taitel–Dukler (1976) model. However, one advantage of the simpler Taitel–Dukler model is that the equations have well-defined limits, and a solution can always be found reliably. Additional refinement of the

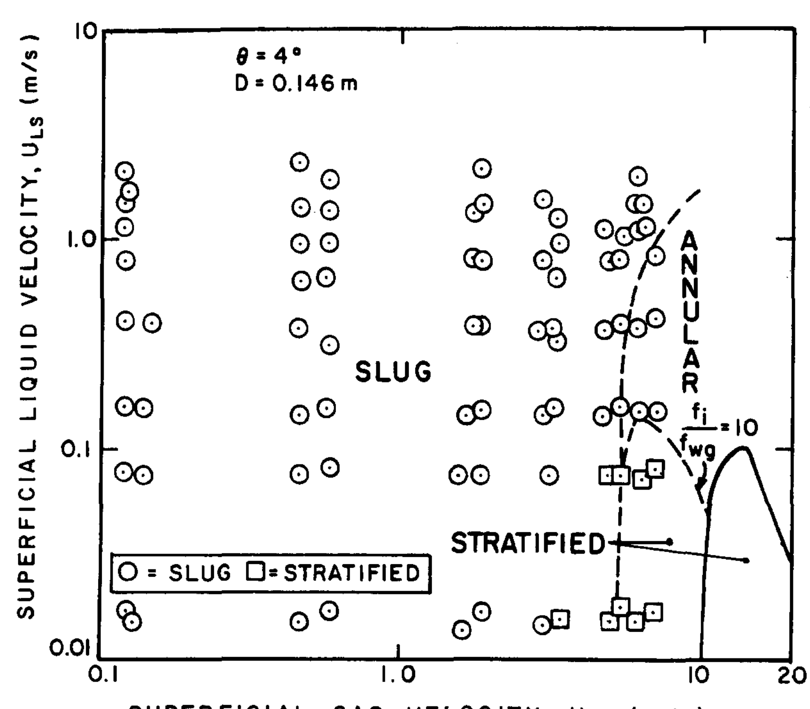

Figure 16. Stratified transition for an upward inclined (°) 0.146 m dia pipe (Ferschneider *et al.* 1985). ——, One-dimensional wave model; – – –, Taitel–Dukler (1976) model.

one-dimensional wave model may be needed before full understanding of its solution characteristics is achieved.

An interesting feature of the one-dimensional wave model is that, unlike the calculation of pressure drop and void fraction in stratified flows, it does not seem to be very sensitive to the interfacial shear. During detailed hand checks of the solutions, it was observed that the terms containing interfacial shear in the equations for the continuity wave velocity are small relative to the liquid shear terms. The interfacial shear does not appear at all in the dynamic wave velocity. Thus, the solution–where the two velocities are equal–is not affected very much by the interfacial shear between the gas and liquid phases.

The basic one-dimensional wave analysis also provides a means to analyze the transient propagation of waves in flow channels. The remainder of this paper describes that application. Information about the frequencies of waves appears in the analysis. Thus, this analysis may also have applications in the prediction of slug frequencies and slug lengths, which is also of interest to multiphase flow calculations in pipes.

5. TRANSIENT ANALYSIS

The criterion developed in section 3 for the stratified-to-slug regime transition defines when instability will occur, but does not allow investigation of its consequences. This may be done using the "method of characteristics", essentially following waves as they grow, decay or intersect. In order to avoid undue complexity, we consider horizontal flow ($\theta = 0°$) and make the assumption that the gas velocity is much larger than the wave speeds of interest, allowing us to drop the time derivatives from [1] and [2]. Equation [1] can then be integrated to give the quasi-steady flow continuity equation for the gas:

$$A_{\mathrm{G}} U_{\mathrm{G}} = A U_{\mathrm{GS}}. \qquad [28]$$

Equation [28] can now be used to substitute for U_{G} whenever it appears. Eliminating P from [2] and [5] we get

$$\frac{\partial h}{\partial x}\left(g\frac{\rho_{\mathrm{L}}-\rho_{\mathrm{G}}}{\rho_{\mathrm{L}}} - \frac{\rho_{\mathrm{G}}}{\rho_{\mathrm{L}}} U_{\mathrm{GS}}^2 \frac{A^2 A_{\mathrm{L}}'}{A_{\mathrm{G}}^3}\right) + \frac{\partial U_{\mathrm{L}}}{\partial t} + U_{\mathrm{L}}\frac{\partial U_{\mathrm{L}}}{\partial x} = -\frac{\tau_{\mathrm{WL}} S_{\mathrm{L}}}{\rho_{\mathrm{L}} A_{\mathrm{L}}} + \frac{\tau_{\mathrm{i}} S_{\mathrm{i}}}{\rho_{\mathrm{L}} A_{\mathrm{L}}} + \frac{1}{\rho_{\mathrm{L}}}\left(\tau_{\mathrm{WG}}\frac{S_{\mathrm{G}}}{A_{\mathrm{G}}} + \frac{\tau_{\mathrm{i}} S_{\mathrm{i}}}{A_{\mathrm{G}}}\right). \qquad [29]$$

We shall denote the right-hand side of [29] by the symbol "f".

Equations [4] and [29] represent two equations for h and U_{L} which may be solved by various methods.

A dimensionless formulation may be obtained by choosing D, the pipe diameter, as the characteristic length that scales all geometrical parameters such as height, width, area, perimeter etc. Dividing [29] by $g(\rho_{\mathrm{L}} - \rho_{\mathrm{G}})/\rho_{\mathrm{L}}$ the dimensionless forms of time, velocity and superficial velocity emerge as

$$t^* = t\left[\frac{g(\rho_{\mathrm{L}} - \rho_{\mathrm{G}})}{D\rho_{\mathrm{L}}}\right]^{1/2}, \qquad [30]$$

$$U_{\mathrm{L}}^* = U_{\mathrm{L}}\left[\frac{\rho_{\mathrm{L}}}{gD(\rho_{\mathrm{L}} - \rho_{\mathrm{G}})}\right]^{1/2}, \qquad [31]$$

$$j_{\mathrm{L}}^* = U_{\mathrm{LS}}\left[\frac{\rho_{\mathrm{L}}}{gD(\rho_{\mathrm{L}} - \rho_{\mathrm{G}})}\right]^{1/2} \qquad [32]$$

and

$$j_{\mathrm{G}}^* = U_{\mathrm{GS}}\left[\frac{\rho_{\mathrm{G}}}{gD(\rho_{\mathrm{L}} - \rho_{\mathrm{G}})}\right]^{1/2}, \qquad [33]$$

The resulting dimensionless forms of [4] and [29], where the variables are all now in their dimensionless form (with "asterisks" and tildes suppressed on geometry and U_L terms for convenience), are

$$\frac{\partial h}{\partial t}+U_L\frac{\partial h}{\partial x}+\frac{A_L}{A_L'}\frac{\partial U_L}{\partial x}=0 \quad [34]$$

$$\frac{\partial h}{\partial x}\left(1-\frac{j_G^{*2}}{\epsilon_G^2}\frac{A_L'}{A_G}\right)+\frac{\partial U_L}{\partial t}+U_L\frac{\partial U_L}{\partial x}=f, \quad [35]$$

where

$$f=-\frac{f_{WL}j_L^{*2}}{2}\frac{S_L}{\epsilon_L^2A_L}+\frac{f_{WG}j_G^{*2}}{2}\frac{S_G}{\epsilon_G^2A_G}+\frac{S_if_i}{2}\left(\frac{1}{A_L}+\frac{1}{A_G}\right)\left[\frac{j_G^{*2}}{\epsilon_G^2}-2\left(\frac{\rho_G}{\rho_L}\right)^{1/2}\frac{j_G^*j_L^*}{\epsilon_L\epsilon_G}+\frac{\rho_Gj_L^{*2}}{\rho_L\epsilon_L^2}\right] \quad [36]$$

and the volume fractions of the phases are

$$\epsilon_L=\frac{4}{\pi}A_L,\quad \epsilon_G=1-\epsilon_L. \quad [37]$$

6. STEADY FLOW—DEVELOPING INTERFACE LEVEL

In steady flow, the time-dependent terms are zero in [34] and [35]. These equations may be solved to determine the height of the interface as a function of location. The result resembles the usual "backwater curves" for open channel flow and describes surface profiles near the inlet and exit, for example. An interesting prediction is the way in which the steady equilibrium depth is approached when the inlet conditions are specified. Under some conditions, a continuous change in depth is unable to link the inlet to the equilibrium depth, and some new phenomenon must occur, such as a change in flow regime. Even if a continuous change in depth is predicted, time-dependent instabilities may still occur; they will be analyzed in subsequent sections.

Removing the $\partial/\partial t$ terms in [34] and [35], we have two equations for dh/dx and dU_L/dx. Eliminating dU_L/dx gives

$$\frac{dh}{dx}\left(1-\frac{j_G^{*2}}{\epsilon_G^2}\frac{A_L'}{A_G}-U_L^2\frac{A_L'}{A_L}\right)=f. \quad [38]$$

The sign of dh/dx depends both on the sign of f and the sign of the term in parentheses. When the term in parentheses is zero, the flow is "critical". The qualitative behavior is very much like that in "open channel flow", with more complicated terms. To provide one interpretation, we can rewrite the term in parentheses as

$$\frac{A_L'}{A_L}(c^2-U_L^2),$$

where

$$c^2=\frac{A_L}{A_L'}\left(1-\frac{j_G^{*2}}{\epsilon_G^2}\frac{A_L'}{A_G}\right), \quad [39]$$

which is the effective wave speed relative to the liquid velocity. Clearly, the effect of the gas flow is to reduce the wave speed, and a sufficiently high gas flux will lead to imaginary wave speeds and rapid instability, if this has not already happened due to some other mechanism.

Equation [39] is an approximation to [24], assuming that $\rho_G \ll \rho_L$ and $U_G \gg U_L$.

7. METHOD OF CHARACTERISTICS

The method of characteristics is a standard approach to solving partial differential equations of the hyperbolic type (i.e. those with real wave velocities). The technique is to find directions in the x–t plane along which the formulation can be recast as ordinary differential equations.

We start by substituting [39] into [35] and adding λ times [34]:

$$\lambda \frac{\partial h}{\partial t} + \frac{\partial h}{\partial x}\left(\lambda U_L + \frac{A'_L}{A_L} c^2\right) + \frac{\partial U_L}{\partial t} + \frac{\partial U_L}{\partial x}\left(U_L + \lambda \frac{A_L}{A'_L}\right) = f; \qquad [40]$$

choosing

$$\lambda = \pm\left(c \frac{A'_L}{A_L}\right), \qquad [41]$$

[40] becomes

$$\pm c \frac{A'_L}{A_L}\left[\frac{\partial h}{\partial t} \pm (U_L \pm c)\frac{\partial h}{\partial x}\right] + \frac{\partial U_L}{\partial t} + (U_L \pm c)\frac{\partial U_L}{\partial x} = f. \qquad [42]$$

The differentials of both h and U_L in [42] are along the "characteristic directions", such that

$$\frac{\mathrm{d}x}{\mathrm{d}t} = U_L \pm c. \qquad [43]$$

We may proceed further by defining

$$y = \int_0^h \frac{c A'_L}{A_L} \mathrm{d}h. \qquad [44]$$

When [44] is used, [42] reduces to the compact form

$$\left[\frac{\partial}{\partial t} + (U_L \pm c)\frac{\partial}{\partial x}\right](U_L \pm y) = f \qquad [45]$$

or

$$\frac{\mathrm{d}}{\mathrm{d}t}(U_L \pm y) = f, \qquad [46]$$

where the differentiation in [46] is along the corresponding direction defined by [43].

The method of characteristics essentially converts the initial partial differential equations into ordinary differential equations. The physical interpretation is that "dynamic waves" travel with the speed given in [43], propagating the effect of initial and boundary conditions. The network of characteristics, or wave paths, in the x–t plane shows how conditions, such as perturbations in depth or velocity, influence the conditions at subsequent times. Numerical methods are usually needed to obtain solutions.

It is easily shown that the stability criterion [27] determines whether waves propagating along characteristic directions will grow or decay. To illustrate this, we ran several examples in which waves of various initial shapes were set up on an equilibrium stratified flow and allowed to propagate. Figure 17(a) shows decaying waves while figure 17(b) shows growing waves. The difference between the two figures lies in the liquid flow rate. The sets of curves correspond to successive shapes of the interface at fixed intervals of the calculation step, corresponding closely to constant intervals of time.

Figure 18 shows more detail of the two "families" of waves described by the two signs in [43]. The waves interact and "pass through" each other. The slower-moving waves decay while the faster-moving waves are approximately neutrally stable. The fact that both sets of waves move downstream indicates that the flow is "supercritical", with $U_L > c$.

Several checks were run on the method. For example, if the inlet condition was set to be a non-equilibrium value of depth, and some form of initial depth variation with x was assumed, the solution near the inlet converged to the developing profile that was calculated separately from the steady flow result [38].

8. SLUG FORMATION AND FREQUENCY

Our formulation retains the gas inertia term neglected by Taitel & Dukler (1977) and should give a fuller description of how waves grow, perhaps eventually to form slugs. The method of

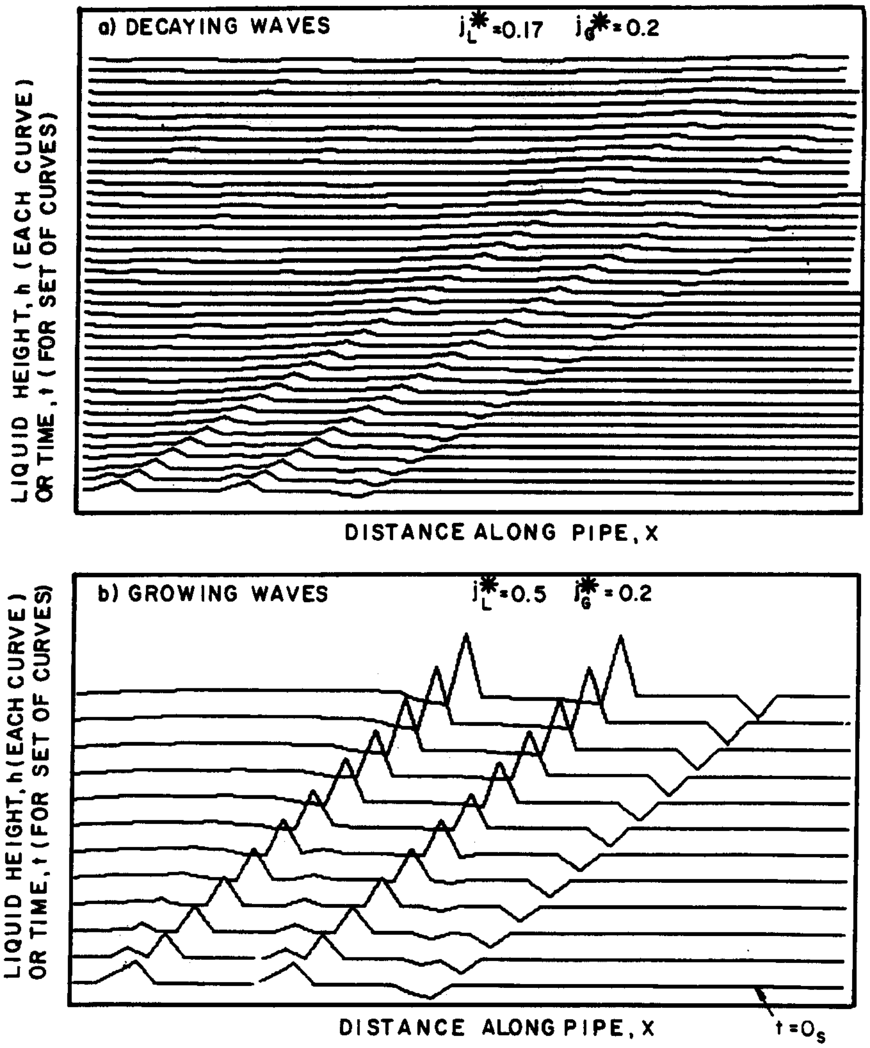

Figure 17. Growth and decay of interfacial waves in stratified flow by the method of characteristics.

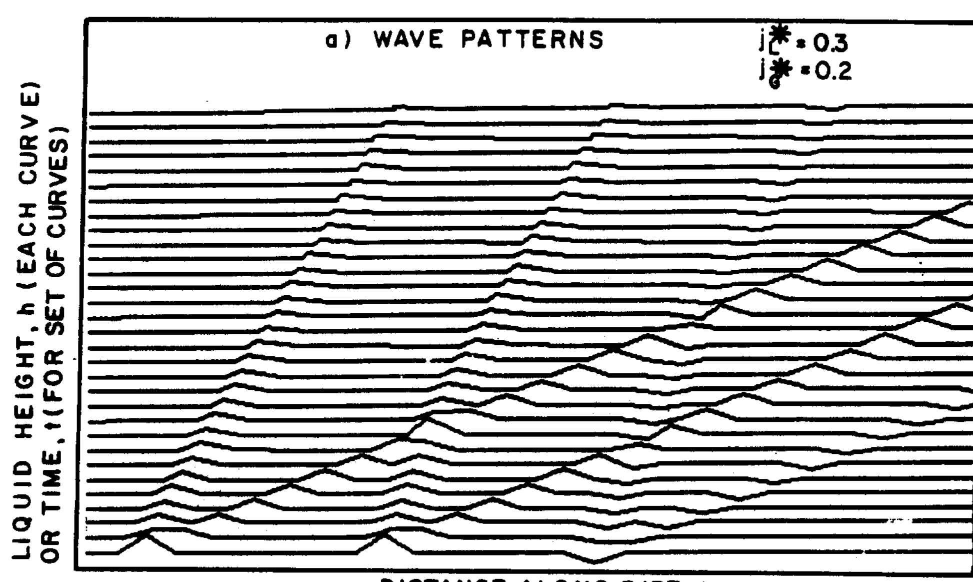

Figure 18. Interaction of interfacial waves in stratified flow by the method of characteristics.

characteristics can be used to follow wave development until c^2 becomes negative, at which time a rapid instability sets in and slugs form.

At first we believed it would be possible to follow the Taitel–Dukler (1977) method, allowing the disturbance left behind by one slug as it was accelerated downstream to grow to form the next one and so on. However, we soon realized that for supercritical stratified flows (which are usually the ones of interest, as Taitel & Dukler mentioned) *all* disturbances propagate downstream and *any* region of slug formation will eventually wash out of the system. After several numerical experiments, we believe the Taitel–Dukler (1977) model to be flawed for this reason.

Our suspicion is that a proper model for slug frequency must incorporate a description of the inlet conditions and compliance. When a new slug forms, it requires additional pressure drop to accelerate it. This feeds back to the inlet by acoustic waves in the gas (which can travel upstream) and changes the conditions there. This new "disturbance" eventually grows to form a slug and the cycle repeats. The method of characteristics can represent this cycle, but assumptions (or a separate mechanistic analysis) are needed about the inlet behavior.

Acknowledgement—The work described in this paper has been sponsored, in part, by the Pipeline Research Committee (PRC). The PRC is an autonomous body within the American Gas Association (AGA) organized in response to the need to sponsor and direct basic, developmental and applied research aimed at optimizing all technical aspects of the natural gas transmission industry and its related activities. Its major activity is the direction of a cooperative research program funded by means of a subscription raised from its individual member companies and carried out under the direct supervision of its individual member-company engineering and technical representatives. Program administration is the responsibility of assigned staffmembers at AGA.

REFERENCES

BARNEA, D., SHOHAM, O., TAITEL, Y. & DUKLER, A. E. 1980 Flow pattern transition for gas–liquid flow in horizontal and inclined pipes. *Int. J. Multiphase Flow* **6,** 217–225.

BARNEA, D., SHOHAM, O. & TAITEL, Y. 1982 Flow pattern transition for downward inclined two-phase flow; horizontal to vertical. *Chem. Engng Sci.* **37,** 735–740.

BENDIKSEN, K., BRANDT, I., FUCHS, P., LINGA, H., MALNES, D. & MOE, R. 1986 Two-phase flow research at SINTEF and IFE: Some experimental results. Presented at the *Offshore Northern Seas Conf.* (ONS 86), Stavanger, Norway.

CROWLEY, C. J. & SAM, R. G. 1986 Investigation of two-phase flow in horizontal and inclined pipes at large pipe size and high gas density. Creare Inc. TN-399, Pipeline Research Committee Project PR 172-507, American Gas Association Catalog No. L51509.

CROWLEY, C. J., IZENSON, M. G. & SAM, R. G. 1988 Scaling of multiphase flow behavior at high gas density. Creare Inc. TN-451, Pipeline Research Committee Project PR 172-811, American Gas Association Catalog No. L51582.

FERSCHNEIDER, G., LAGIERE, M., BOURGEOIS, T. & FITREMANN, J-M. 1985 How to calculate two-phase flow of gas and oil in pipe lines. *Pipe Line Ind.* **63,** 33–39.

JEPSON, W. P. 1989 Modelling the transition to slug flow in a horizontal conduit. *Can. J. Chem. Engng* **67,** 731–740.

JEPSON, W. P., TAYLOR, R. E. & EVANS, N. 1989 Slug flow and its transitions in large diameter horizontal pipes. Harwell Labs Report AERE R-12992 (Revision 1).

KORDYBAN, E. S. & RANOV, T. 1970 Mechanisms of slug formation in horizontal two-phase flow. *J. Bas. Engng Trans. ASME* **92,** 857–864.

KOUBA, G. E. & JEPSON, W. P. 1989 The flow of slugs in horizontal, two-phase pipelines, Harwell Labs Report AERE R-13269.

LIN, J. C. & HANRATTY, T. J. 1986 Prediction of the initiation of slugs with linear stability theory. *Int. J. Multiphase Flow* **12,** 79–98.

SIMPSON, H. C. 1981 Two-phase flow studies in large diameter horizontal tubes. National Engineering Lab. Report NEL-677, Univ. of Strathclyde, East Kilbride, Glasgow, Scotland.

TAITEL, Y. & DUKLER, A. E. 1976 A model for predicting flow regime transitions in horizontal and near horizontal gas–liquid flow. *AIChE JL* **22,** 47–56.

TAITEL, Y. & DUKLER, A. E. 1977 A model for slug frequency during gas–liquid flow in horizontal and near-horizontal pipes. *Int. J. Multiphase Flow* **3,** 585–596.

WALLIS, G. B. 1969 *One-dimensional Two-phase Flow*. McGraw-Hill, New York.

WALLIS, G. B. & DOBSON, J. E. 1973 The onset of slugging in horizontal, stratified air–water flow. *Int. J. Multiphase Flow* **1**, 173–193.

WU, H. L., POTS, B. F. M., HOLLENBERG, J. F. & MEERHOFF, R. 1987 Flow pattern transitions in a two-phase gas/condensate flow at high pressure in an 8″ horizontal pipe. In *Proc. 3rd Int. Conf. on Multi-phase Flow*, The Hague, The Netherlands, pp. 13–21.